

LATTICE REALIZATIONS OF UNITARY MINIMAL MODULAR INVARIANT PARTITION FUNCTIONS

David L. O'Brien¹ and Paul A. Pearce²

*Mathematics Department, University of Melbourne,
Parkville, Victoria 3052, Australia*

Abstract

The conformal spectra of the critical dilute $A-D-E$ lattice models is studied numerically. The results strongly indicate that, in branches 1 and 2, these models provide realizations of the complete $A-D-E$ classification of unitary minimal modular invariant partition functions given by Cappelli, Itzykson and Zuber. In branches 3 and 4 the results indicate that the modular invariant partition functions factorize. Similar factorization results are also obtained for two-colour lattice models.

1 Introduction

It is well established that the critical behaviour of two-dimensional lattice models is described by conformal field theory or, to put it another way, that the continuum limit of critical lattice models provide realizations of two-dimensional conformal field theories. An important class of conformal field theories is the unitary minimal series with central charge $c < 1$. In this case a complete $A-D-E$ classification of the theories has been obtained by Cappelli, Itzykson and Zuber [1]. In this paper we present compelling numerical evidence to show that the critical dilute $A-D-E$ lattice models provide realizations of this complete $A-D-E$ classification of unitary minimal conformal field theories. The layout of the paper is as follows. In Section 2 we describe the minimal conformal field theories and their $A-D-E$ classification. In Section 3 we define the critical $A-D-E$ models due to Pasquier [2] and their dilute [3, 4, 5] and two-colour [6] generalizations. We also summarize the conjectured modular invariant partition functions for these models. Finally, in Section 4, we present the numerical results that confirm the conjectured modular invariant partition functions.

2 Conformal Field Theory

2.1 Minimal Models

Ten years ago, in 1984, Belavin, Polyakov and Zamolodchikov [7] introduced the minimal series of conformally invariant field theories. These models are characterized by a central

¹Email: dlo@mundoe.maths.mu.oz.au

²Email: pap@mundoe.maths.mu.oz.au

charge $c < 1$ which is restricted to the discrete values

$$c = 1 - \frac{6(p-p')^2}{pp'} \quad (2.1)$$

with p and p' coprime positive integers. The conformal weights of the minimal series are given by the Kac formula

$$\Delta = \Delta_{r,s}^{(p,p')} = \frac{(rp' - sp)^2 - (p' - p)^2}{4pp'} \quad (2.2)$$

with

$$1 \leq r \leq p-1, \quad 1 \leq s \leq p'-1. \quad (2.3)$$

Moreover, Friedan, Qiu and Shenker [8] showed that if the theory is unitary, which is required for the theory to be physical, then the central charge is further restricted by $|p - p'| = 1$, that is,

$$c = 1 - \frac{6}{h(h-1)}, \quad h = 4, 5, 6, \dots \quad (2.4)$$

where $h = \max(p, p')$. The grids of conformal weights for $h = 4, 5$ and 6 are shown in Figure 1.

		$h = 4$	
s			
3		1/2	0
2		1/16	1/16
1		0	1/2
		1	2
			r

		$h = 5$		
s				
4		3/2	7/16	0
3		3/5	3/80	1/10
2		1/10	3/80	3/5
1		0	7/16	3/2
		1	2	3
				r

		$h = 6$			
s					
5		3	7/5	2/5	0
4		13/8	21/40	1/40	1/8
3		2/3	1/15	1/15	2/3
2		1/8	1/40	21/40	13/8
1		0	2/5	7/5	3
		1	2	3	4
					r

Figure 1. Conformal grids of conformal weights for the unitary minimal models with $h = 4, 5, 6$. The table with $h = 4$, $c = 1/2$ is identified with the Ising model, $h = 5$, $c = 7/10$ is identified with the tricritical Ising model and $h = 6$, $c = 4/5$ with the tetracritical Ising model. The odd rows of the $h = 6$ Kac table give the critical exponents of the 3-state Potts model.

2.2 A - D - E Classification of Modular Invariant Partition Functions

For a conformal field theory on a torus, modular invariance [9] implies further constraints on the theory. The requirement of modular invariance is strong enough to fix the operator content. In fact, Cappelli, Itzykson and Zuber [1] have obtained a complete classification of minimal modular invariant partition functions. Remarkably they obtain two series in one-to-one correspondence with the A - D - E classical Lie algebras. The A - D - E classification of minimal modular invariant partition functions, as given by Cappelli, Itzykson and Zuber, is shown in Table 1. The Virasoro characters in this table are defined by

$$\begin{aligned}\chi_{r,s}(q) &= \text{Virasoro character of } G' \\ &= \frac{q^{-c/24+\Delta_{r,s}^{(p,p')}}}{Q(q)} \sum_{n=-\infty}^{\infty} \left\{ q^{n(npp' + rp' - sp)} - q^{(np' + s)(np + r)} \right\}\end{aligned}\quad (2.5)$$

where q is the modular parameter and

$$Q(q) = \prod_{n=1}^{\infty} (1 - q^n). \quad (2.6)$$

Here we are primarily interested in the unitary minimal models with $p' - p = \pm 1$. In this case there are two A - D - E series where

$$(r, s) = \text{Coxeter exponents of } (G, G'), \quad (2.7)$$

$$(A, G') = \begin{cases} (A_{h-2}, A_{h-1}) \\ (A_{h-2}, D_{(h+2)/2}) \\ (A_{10}, E_6) \\ (A_{16}, E_7) \\ (A_{28}, E_8) \end{cases} \quad (G, A') = \begin{cases} (A_{h-1}, A_h) \\ (D_{(h+2)/2}, A_h) \\ (E_6, A_{12}) \\ (E_7, A_{18}) \\ (E_8, A_{30}) \end{cases} \quad (2.8)$$

and

$$c = c(G') = 1 - \frac{6}{h(h-1)}. \quad (2.9)$$

The Coxeter number $h = \max(p, p')$ and the Coxeter exponents s of the classical A - D - E Lie algebras are shown in Table 2. The Dynkin diagrams are shown in Figure 2. Some members of these series are identified as follows:

$$\begin{aligned}(A_2, A_3) &= \text{critical Ising} & c &= 1/2 \\ (A_4, D_4) &= \text{critical 3-state Potts} & c &= 4/5 \\ (A_3, A_4) &= \text{tricritical Ising} & c &= 7/10 \\ (D_4, A_6) &= \text{tricritical 3-state Potts} & c &= 6/7\end{aligned}\quad (2.10)$$

For this reason we will refer to the (A, G') series as the critical series and the (G, A') series as the tricritical series. In particular, the modular invariant partition functions of

(G, G')	Modular Invariant Partition Function
$(A_{p-1}, A_{p'-1})$	$Z = \frac{1}{2} \sum_{r=1}^{p-1} \sum_{s=1}^{p'-1} \chi_{r,s} ^2$
$(A_{p-1}, D_{2\rho+2})$ $p'=4\rho+2 \geq 6$	$Z = \frac{1}{2} \sum_{r=1}^{p-1} \left\{ \sum_{\substack{s=1 \\ s \text{ odd}}}^{2\rho-1} \chi_{r,s} + \chi_{r,4\rho+2-s} ^2 + 2 \chi_{r,2\rho+1} ^2 \right\}$
$(A_{p-1}, D_{2\rho+1})$ $p'=4\rho \geq 8$	$Z = \frac{1}{2} \sum_{r=1}^{p-1} \left\{ \sum_{\substack{s=1 \\ s \text{ odd}}}^{4\rho-1} \chi_{r,s} ^2 + \chi_{r,2\rho} ^2 + \sum_{\substack{s=2 \\ s \text{ even}}}^{2\rho-2} (\chi_{r,s} \bar{\chi}_{r,4\rho-s} + \bar{\chi}_{r,s} \chi_{r,4\rho-s}) \right\}$
(A_{p-1}, E_6) $p'=12$	$Z = \frac{1}{2} \sum_{r=1}^{p-1} \left\{ \chi_{r,1} + \chi_{r,7} ^2 + \chi_{r,4} + \chi_{r,8} ^2 + \chi_{r,5} + \chi_{r,11} ^2 \right\}$
(A_{p-1}, E_7) $p'=18$	$Z = \frac{1}{2} \sum_{r=1}^{p-1} \left\{ \chi_{r,1} + \chi_{r,17} ^2 + \chi_{r,5} + \chi_{r,13} ^2 + \chi_{r,7} + \chi_{r,11} ^2 \right.$ $\left. + \chi_{r,9} ^2 + [(\chi_{r,3} + \chi_{r,15})\bar{\chi}_{r,9} + (\bar{\chi}_{r,3} + \bar{\chi}_{r,15})\chi_{r,9}] \right\}$
(A_{p-1}, E_8) $p'=30$	$Z = \frac{1}{2} \sum_{r=1}^{p-1} \left\{ \chi_{r,1} + \chi_{r,11} + \chi_{r,19} + \chi_{r,29} ^2 \right.$ $\left. + \chi_{r,7} + \chi_{r,13} + \chi_{r,17} + \chi_{r,23} ^2 \right\}$

Table 1. A - D - E classification of minimal modular invariant partition functions. The central charges are $c = c(G') = 1 - \frac{6(p-p')^2}{pp'}$, $\chi_{r,s} = \chi_{r,s}(q)$ are Virasoro characters and bars denote complex conjugates. In this series r, s are Coxeter exponents of (A, G') and $p' > p$. There is a second series where r, s are Coxeter exponents of (G, A') . The unitary minimal models have $|p - p'| = 1$.

the critical and tricritical 3-state Potts models are

$$(A_4, D_4) : \quad Z = \frac{1}{2} \sum_{r=1}^4 \left\{ |\chi_{r,1} + \chi_{r,5}|^2 + 2|\chi_{r,3}|^2 \right\} \quad (p = 5, p' = 6) \quad (2.11)$$

$$(D_4, A_6) : \quad Z = \frac{1}{2} \sum_{s=1}^6 \left\{ |\chi_{1,s} + \chi_{5,s}|^2 + 2|\chi_{3,s}|^2 \right\} \quad (p = 7, p' = 6). \quad (2.12)$$

The A - D - E classification of unitary minimal conformal field theories gives an exhaustive list of theories with $c < 1$. In other words, this is a complete list of universality classes giving all possible critical behaviours for two-dimensional statistical systems with $c < 1$. A natural question to ask is whether a solvable lattice model can be found as a representative of each universality class allowed by the A - D - E classification.

G	h	s
A_L	$L + 1$	$1, 2, 3, \dots, L$
D_L	$2L - 2$	$L - 1, 1, 3, 5, \dots, 2L - 3$
E_6	12	$1, 4, 5, 7, 8, 11$
E_7	18	$1, 5, 7, 9, 11, 13, 17$
E_8	30	$1, 7, 11, 13, 17, 19, 23, 29$

Table 2. The Coxeter number h and Coxeter exponents s of the classical A - D - E Lie algebras.

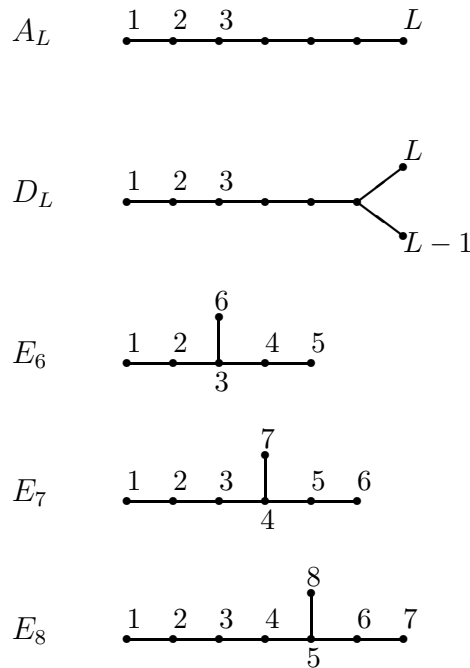


Figure 2. The Dynkin diagrams of the classical A - D - E Lie algebras. The A - D - E graphs classify all graphs whose associated adjacency matrices have eigenvalues strictly less than 2. The eigenvalues of the adjacency matrices are in fact given by $2 \cos(s\pi/h)$ where s ranges over the Coxeter exponents.

3 A - D - E Lattice Models and Their Modular Invariant Partition Functions

3.1 Pasquier's A - D - E Models

By a remarkable coincidence, in the same year that Belavin, Polyakov and Zamolodchikov introduced the minimal conformal field theories, Andrews, Baxter and Forrester [10] solved the first infinite hierarchy of lattice models in the form of restricted solid-on-solid (RSOS) models. The spins in these models take values on the A_L Dynkin diagram and are subject to the constraint that the state of adjacent spins on the square lattice must be adjacent on the A_L diagram. Huse [11] showed that the critical behaviour of these L height RSOS models is precisely described by the unitary minimal series. Moreover, it turns out that the modular invariant partition functions of the ABF RSOS models give the (A_{L-1}, A_L) series with $L = 3, 4, 5, \dots$

The lattice realizations of this critical series of modular invariant partition functions was completed in 1987 by Pasquier [2] who generalized the ABF models by constructing solvable lattice models whose states take values on the A - D - E graphs. The A_L models of Pasquier are just the critical ABF RSOS models. We note that, although the A and D models admit off-critical elliptic extensions, the exceptional E models can only be solved at criticality. The face weights of Pasquier's critical A - D - E models are given by

$$W \left(\begin{array}{cc|c} d & c & \\ \hline & u & \\ \hline a & b & \end{array} \right) = \begin{array}{c} d \quad c \\ \hline \square \\ \hline a \quad b \end{array} = \frac{\sin(\lambda - u)}{\sin \lambda} \delta_{a,c} A_{a,b} A_{a,d} + \frac{\sin u}{\sin \lambda} \sqrt{\frac{S_a S_c}{S_b S_d}} \delta_{b,d} A_{a,b} A_{b,c} \quad (3.1)$$

where the spins a, b, c, d take values on the given A - D - E graph. The parameter u is called the spectral parameter. In the branches of interest here the spectral parameter lies in the interval $0 < u < \lambda$. The adjacency matrices are given by

$$A_{a,b} = \begin{cases} 1, & a, b \text{ connected} \\ 0, & \text{otherwise.} \end{cases} \quad (3.2)$$

The nonnegative components S_a of the Perron-Frobenius eigenvector are determined by

$$\sum_b A_{a,b} S_b = 2 \cos \lambda S_a \quad (3.3)$$

where $2 \cos \lambda$ is the largest eigenvalue of the adjacency matrix and

$$\lambda = \pi/h \quad (3.4)$$

is called the crossing parameter. The Coxeter number h is given in Table 2.

Pasquier's A - D - E models include some much studied models in statistical mechanics. Some prototypes are shown in Figure 3. The modular invariant partition functions of Pasquier's critical A - D - E models precisely realize the (A, G') series of Cappelli, Itzykson and Zuber. However, for many years realizations of the (G, A') series were missing.

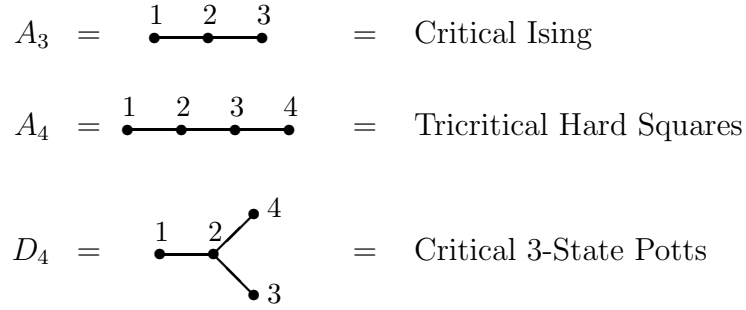


Figure 3. Some prototype classical A - D - E lattice models.

3.2 Dilute A - D - E Models

In 1992 Warnaar, Nienhuis and Seaton [3] and Roche [4] independently obtained a second series of solvable lattice models whose states take values on the A - D - E graphs. These lattice models are called the dilute A - D - E models. The face weights of the dilute A - D - E lattice models at criticality are given by

$$\begin{aligned}
W \left(\begin{array}{c|c} d & c \\ a & b \end{array} \middle| u \right) &= \rho_1(u) \delta_{a,b,c,d} + \rho_2(u) \delta_{a,b,c} A_{a,d} + \rho_3(u) \delta_{a,c,d} A_{a,b} \\
&+ \sqrt{\frac{S_a}{S_b}} \rho_4(u) \delta_{b,c,d} A_{a,b} + \sqrt{\frac{S_c}{S_a}} \rho_5(u) \delta_{a,b,d} A_{a,c} + \rho_6(u) \delta_{a,b} \delta_{c,d} A_{a,c} \\
&+ \rho_7(u) \delta_{a,d} \delta_{c,b} A_{a,b} + \rho_8(u) \delta_{a,c} A_{a,b} A_{a,d} + \sqrt{\frac{S_a S_c}{S_b S_d}} \rho_9(u) \delta_{b,d} A_{a,b} A_{b,c}
\end{aligned} \tag{3.5}$$

where, as before, the adjacency matrix is

$$A_{a,b} = \begin{cases} 1, & a, b \text{ adjacent} \\ 0, & \text{otherwise} \end{cases} \tag{3.6}$$

and the Perron-Frobenius vector is given by

$$\sum_b A_{a,b} S_b = 2 \cos \left(\frac{\pi}{h} \right) S_a. \tag{3.7}$$

The effective adjacency graph is given by adding a loop to each node of the A - D - E graphs, that is, the spin states at adjacent sites of the lattice are either the same or adjacent on the A - D - E graph. The generalized Kronecker delta is

$$\delta_{a,b,c,\dots} = \begin{cases} 1, & a = b = c = \dots \\ 0, & \text{otherwise} \end{cases} \tag{3.8}$$

and the trigonometric functions are

$$\begin{aligned}
\rho_1(u) &= 1 + \frac{\sin u \sin(3\lambda - u)}{\sin(2\lambda) \sin(3\lambda)} \\
\rho_2(u) &= \rho_3(u) = \frac{\sin(3\lambda - u)}{\sin(3\lambda)}
\end{aligned}$$

$$\begin{aligned}
\rho_4(u) &= \rho_5(u) = \frac{\sin u}{\sin(3\lambda)} \\
\rho_6(u) &= \rho_7(u) = \frac{\sin u \sin(3\lambda - u)}{\sin(2\lambda) \sin(3\lambda)} \\
\rho_8(u) &= \frac{\sin(2\lambda - u) \sin(3\lambda - u)}{\sin(2\lambda) \sin(3\lambda)} \\
\rho_9(u) &= -\frac{\sin u \sin(\lambda - u)}{\sin(2\lambda) \sin(3\lambda)}.
\end{aligned} \tag{3.9}$$

The dilute A - D - E models are solvable for two choices of λ

$$\lambda = \begin{cases} \frac{(h-1)\pi}{4h}, & \text{branches 1 and 4} \\ \frac{(h+1)\pi}{4h}, & \text{branches 2 and 3.} \end{cases} \tag{3.10}$$

The physical branches are summarised in Table 3. The central charges of these models in branches 1 and 2 are given by [12, 5, 13]

$$c = \begin{cases} 1 - \frac{6}{h(h+1)}, & \text{branch 1} \\ 1 - \frac{6}{h(h-1)}, & \text{branch 2.} \end{cases} \tag{3.11}$$

This suggests identifying the universality classes of the first few dilute A - D - E models as follows:

$$\begin{aligned}
\text{branch 2: } A_3 &= \text{critical Ising} & c &= 1/2 \\
\text{branch 1: } A_3 &= \text{tricritical Ising} & c &= 7/10 \\
\text{branch 2: } D_4 &= \text{critical 3-state Potts} & c &= 4/5 \\
\text{branch 1: } D_4 &= \text{tricritical 3-state Potts} & c &= 6/7
\end{aligned} \tag{3.12}$$

Notice that the dilute A_3 and D_4 are not the usual Ising and 3-state Potts models, they just have the same \mathbf{Z}_2 and \mathbf{Z}_3 symmetries and lie in the same universality classes.

The dilute A - D - E lattice models in branch 2 in fact give a second realization of the (A, G') series of Cappelli, Itzykson and Zuber. More importantly, as we show in the next section, the dilute A - D - E lattice models in branch 1 precisely realize the missing (G, A') series. The dilute A - D - E models thus give a complete realization of all unitary minimal conformal field theories.

	Crossing param.	Inversion pt	Phys. region	Central charge
Branch 1	$\lambda = \frac{\pi}{4} \left(1 - \frac{1}{h}\right)$	$\gamma = 3\lambda$	$u \in (0, \gamma)$	$c = 1 - \frac{6}{h(h+1)}$
Branch 2	$\lambda = \frac{\pi}{4} \left(1 + \frac{1}{h}\right)$	$\gamma = 3\lambda$	$u \in (0, \gamma)$	$c = 1 - \frac{6}{h(h-1)}$
Branch 3	$\lambda = \frac{\pi}{4} \left(1 + \frac{1}{h}\right)$	$\gamma = 3\lambda - \pi$	$u \in (\gamma, 0)$	$c = \frac{3}{2} - \frac{6}{h(h+1)}$
Branch 4	$\lambda = \frac{\pi}{4} \left(1 - \frac{1}{h}\right)$	$\gamma = 3\lambda - \pi$	$u \in (\gamma, 0)$	$c = \frac{3}{2} - \frac{6}{h(h-1)}$

Table 3. Physical branches and central charges of the dilute A - D - E lattice models

3.3 Two-Colour A-D-E Models

The two-colour models, obtained by Warnaar and Nienhuis [6], are dense RSOS models built on pairs of A-D-E adjacency graphs. Each site on the lattice carries two heights, one from each graph. In moving between adjacent sites, one of the heights remains constant and the other varies as permitted by its corresponding adjacency graph. If G^1 and G^2 are the adjacency matrices of the two graphs, the effective adjacency matrix of the two-colour model is therefore $A = A^1 + A^2$, where

$$A^1 = G^1 \otimes I, \quad A^2 = I \otimes G^2 \quad (3.13)$$

With a slight abuse of notation we will denote such a model by $G^1 \otimes G^2$. The Perron-Frobenius vector of A is the tensor product $S = S^1 \otimes S^2$ of the Perron-Frobenius vectors of the underlying graphs. In constructing the two-colour models it is assumed that the graphs G^1 and G^2 have the same largest eigenvalue and hence the same Coxeter numbers.

Explicitly, the state at each site is given by an ordered pair $a = (a_1, a_2)$ so that

$$S_a = S_{a_1}^1 S_{a_2}^2 \quad (3.14)$$

$$A_{a,b}^i = G_{a_i, b_i}^i \delta_{a_{3-i}, b_{3-i}}. \quad (3.15)$$

In terms of these entities, the face weights of the critical lattice model are given by

$$\begin{aligned} W \left(\begin{array}{c|c} d & c \\ a & b \end{array} \middle| u \right) &= \sum_{i=1}^2 \left[\rho_1(u) A_{a,b}^i A_{b,c}^{3-i} A_{c,d}^i A_{d,a}^{3-i} \right. \\ &+ \delta_{a,c} \left(\rho_2(u) A_{a,b}^i A_{a,d}^i + \rho_3(u) A_{a,b}^i A_{a,d}^{3-i} \right) \\ &\left. + \sqrt{\frac{S_a S_c}{S_b S_d}} \delta_{b,d} \left(\rho_4(u) A_{a,b}^i A_{b,c}^{3-i} + \rho_5(u) A_{a,b}^{3-i} A_{b,c}^i \right) \right] \end{aligned} \quad (3.16)$$

where

$$\begin{aligned} \rho_1(u) &= \epsilon \frac{\sin u \sin(3\lambda - u)}{\sin \lambda \sin 3\lambda} \\ \rho_2(u) &= \frac{\sin(\lambda - u) \sin(3\lambda - u)}{\sin \lambda \sin 3\lambda} \\ \rho_3(u) &= \frac{\sin(3\lambda - u)}{\sin 3\lambda} \\ \rho_4(u) &= -\frac{\sin u \sin(2\lambda - u)}{\sin \lambda \sin 3\lambda} \\ \rho_5(u) &= -\epsilon \frac{\sin u}{\sin 3\lambda} \end{aligned} \quad (3.17)$$

	Crossing param.	Inversion pt	Phys. region	Central charge
Branch 1	$\lambda = \frac{\pi}{2} \left(1 - \frac{1}{h}\right)$	$\gamma = 3\lambda - \pi$	$u \in (0, \gamma)$	$c = 2 \left(1 - \frac{6}{h(h+1)}\right)$
Branch 2	$\lambda = \frac{\pi}{2} \left(1 - \frac{1}{h}\right)$	$\gamma = 3\lambda - 2\pi$	$u \in (\gamma, 0)$	$c = 2 \left(1 - \frac{6}{h(h-1)}\right)$

Table 4. Physical branches and central charges of the two-colour $C_2^{(1)}$ RSOS models

The two-colour models have two physical regimes as summarised in Table 4. The choice of the sign factor $\epsilon = \pm 1$ such that $\epsilon = 1$ in branch 1 and $\epsilon = -1$ in branch 2 ensures that the Boltzmann weights are positive.

3.4 Conjectured Modular Invariant Partition Functions

The partition function of a critical lattice model on a finite $\ell \times \ell'$ periodic lattice or torus can be written as

$$Z_{\ell, \ell'} \sim \exp(-\ell \ell' f) Z(q) \quad (3.18)$$

where f is the bulk free energy and $Z(q)$ is a universal term describing the leading finite-size corrections in the limit of ℓ, ℓ' large with the aspect ratio $\delta = \ell'/\ell$ fixed. The argument q is the modular parameter. For a spatially isotropic model, it is simply related to the aspect ratio δ by $q = \exp(-2\pi\delta)$.

The modular invariant partition functions of the dilute A - D - E models are conjectured to be as follows:

$$\begin{aligned} \text{Branch 1:} & (G, A_h) \\ \text{Branch 2:} & (A_{h-2}, G) \\ \text{Branch 3:} & (G, A_h) \times (A_2, A_3) \\ \text{Branch 4:} & (A_{h-2}, G) \times (A_2, A_3). \end{aligned}$$

Here the modular parameter is

$$q = \exp(2\pi i\tau), \quad \tau = \frac{\ell'}{\ell} \exp[i(\pi - \theta)] \quad (3.19)$$

and the effective angle θ [14] is given by

$$\theta = \begin{cases} \frac{\pi u}{3\lambda}, & \text{branches 1 and 2} \\ \frac{\pi u}{3\lambda - \pi}, & \text{branches 3 and 4.} \end{cases} \quad (3.20)$$

The modular invariant partition functions of the two-colour $C_2^{(1)}$ RSOS models are conjectured to be as follows:

$$\begin{aligned} \text{Branch 1:} & (G, A_h) \times (G', A_h) \\ \text{Branch 2:} & (A_{h-2}, G) \times (A_{h-2}, G'). \end{aligned}$$

Here the modular parameter q is as before but now the effective angle is

$$\theta = \begin{cases} \frac{\pi u}{3\lambda - \pi}, & \text{branch 1} \\ \frac{\pi u}{3\lambda - 2\pi}, & \text{branch 2.} \end{cases} \quad (3.21)$$

4 Numerical Results

The central charges and scaling dimensions of critical lattice models can be extracted [15] from the finite-size corrections to the eigenvalues of the row transfer matrices

$$\langle \mathbf{a} | \mathbf{T}(u) | \mathbf{b} \rangle = \prod_{j=1}^N W \left(\begin{array}{cc} b_j & b_{j+1} \\ a_j & a_{j+1} \end{array} \middle| u \right). \quad (4.1)$$

Specifically, the finite-size corrections to the largest eigenvalue Λ_0 of a periodic transfer matrix with N faces take the form

$$\frac{1}{N} \log \Lambda_0(u) = -f(u) + \frac{\pi c}{6N^2} \sin \theta(u) + o\left(\frac{1}{N^2}\right), \quad (4.2)$$

where f is the free energy, c is the central charge and $\theta(u)$ is the effective angle as defined in Section 3.4. At an isotropic point for a square ordered phase u is fixed such that $\theta = \pi/2$. The finite-size corrections to the next-largest eigenvalues Λ_n with $n = 1, 2, 3, \dots$ take the form

$$\frac{1}{N} \log \Lambda_n(u) = -f(u) + \frac{2\pi}{N^2} \left[\left(\frac{c}{12} - x_n \right) \sin \theta(u) - i s_n \cos \theta(u) \right] + o\left(\frac{1}{N^2}\right), \quad (4.3)$$

where $x_n = \Delta + \bar{\Delta}$ and $s_n = \Delta - \bar{\Delta}$ are respectively the scaling dimension and spin. The scaling dimension takes fractional values whereas the spin is restricted to integer values.

The free energies of the dilute and two-colour models are calculated by solving the appropriate inversion relations

$$\kappa(u)\kappa(-u) = \rho(u)\rho(-u), \quad \kappa(u) = \kappa(\gamma - u) \quad (4.4)$$

where $f(u) = -\log \kappa(u)$ is the free energy and

$$\rho(u) = \begin{cases} \frac{\sin(2\lambda - u) \sin(3\lambda - u)}{\sin 2\lambda \sin 3\lambda}, & \text{dilute models} \\ \frac{\sin(2\lambda - u) \sin(6\lambda - u)}{\sin 2\lambda \sin 6\lambda}, & \text{two-colour models.} \end{cases} \quad (4.5)$$

The free energy of the critical dilute models is given by [5]

$$f(u) = -2 \int_{-\infty}^{\infty} \frac{\cosh(\pi - 5\lambda)x \cosh \lambda x \sinh(\gamma - u)x \sinh ux}{x \sinh \pi x \cosh \gamma x} dx \quad (4.6)$$

and the free energy of the critical two-colour models is given by

$$f(u) = -2 \int_{-\infty}^{\infty} \frac{\cosh(\pi - 2\lambda)x \cosh 2(\pi - 2\lambda)x \sinh(\gamma - u)x \sinh ux}{x \sinh \pi x \cosh \gamma x} dx. \quad (4.7)$$

In these expressions γ is the inversion point in the appropriate branch. The dilute and two-colour models have respectively four and two critical branches. Tables 3 and 4 summarise the crossing parameters, inversion points and central charges in each of the physical branches in terms of the Coxeter numbers h of the underlying graphs as given in Table 2.

Model	Branch 1			Branch 2			N_{\max}
	Approx.	Exact		Approx.	Exact		
A_3	0.699999	7/10	0.7	0.500000	1/2	0.5	12
A_4	0.799997	4/5	0.8	0.699997	7/10	0.7	10
A_5, D_4	0.857140	6/7	0.857143...	0.799997	4/5	0.8	10
A_7, D_5	0.916660	11/12	0.916666...	0.892849	25/28	0.892857...	9
A_{11}, D_7, E_6	0.961531	25/26	0.961538...	0.954536	21/22	0.954545...	9
A_{17}, D_{10}, E_7	0.982448	56/57	0.982456...	0.980383	50/51	0.980392...	9

Table 5. Central charges of the dilute A - D - E lattice models in the $u > 0$ branches.

Model	Branch 3			Branch 4			N_{\max}
	Approx.	Exact		Approx.	Exact		
A_3	1.232	6/5	1.2	1.000	1	1	12
A_4	1.327	13/10	1.3	1.199	6/5	1.2	10
A_5, D_4	1.377	19/14	1.357...	1.299	13/10	1.3	10
A_7, D_5	1.432	17/12	1.417...	1.391	39/28	1.393...	8
A_{11}, D_7, E_6	1.470	19/13	1.462...	1.453	16/11	1.455...	8
A_{17}, D_{10}, E_7	1.487	169/114	1.482...	1.479	151/102	1.480...	8

Table 6. Central charges of the dilute A - D - E lattice models in the $u < 0$ branches.

Given the free energy, the central charge c is estimated by calculating a sequence of largest eigenvalues Λ_0 for increasing values of N and applying a suitable extrapolation scheme. Once the central charge is determined, (4.3) then allows estimation of the scaling dimensions by a similar procedure using the next-largest eigenvalues Λ_n . To obtain accurate values for the central charges and scaling dimensions we need to calculate eigenvalues for N as large as possible. It is therefore convenient to prediagonalize the transfer matrices into block diagonal form using the eigenvectors of the shift operator $\Omega = \mathbf{T}(0)$ and, in the case of the A and D models, the reflection operator \mathbf{R} which arises from the \mathbf{Z}_2 symmetry of the A and D Dynkin diagrams. Taken together, these operators reduce the transfer matrices to $2N$ diagonal blocks.

Once a sequence of eigenvalues for increasing N is obtained, equations (4.2) and (4.3) imply that, for large N , the graph of $(\log \Lambda_n/N + f)$ against $1/N^2$ should approximate a line through the origin. However, since the $\mathcal{O}(N^{-2})$ corrections tend to vanish fairly slowly, a parabolic fit gives better results. A simple extrapolation scheme to extract the $1/N$ term is to discard all but the last two eigenvalues in the sequence and take the linear coefficient of the parabola passing through these two points and the origin. We have performed this calculation to find numerically the central charges of a variety of dilute and two-colour models as well as the scaling dimensions of the dilute A_3 , A_4 , D_4 , and two-colour $A_4 \otimes A_4$ models. The approximate central charges are summarised in Tables 5 to 7 and the approximate scaling dimensions are summarised in Tables 8 to 14.

The estimates of the scaling dimensions allow the first few terms of the isotropic modular invariant partition functions to be determined. For the dilute models, we see that branches 1 and 2 are described by the series of partition functions in Table 1 and

that the partition functions in branches 3 and 4 are the product of the critical Ising partition function (A_2, A_3) with those of branches 1 and 2 respectively.

Dilute A_3 therefore has the following modular invariant partition functions in its four branches:

$$\begin{aligned} \text{Branch 1: } & (A_3, A_4) \\ \text{Branch 2: } & (A_2, A_3) \\ \text{Branch 3: } & (A_3, A_4) \times (A_2, A_3) \\ \text{Branch 4: } & (A_2, A_3) \times (A_2, A_3) \end{aligned}$$

Similarly, dilute A_4 has the partition functions

$$\begin{aligned} \text{Branch 1: } & (A_4, A_5) \\ \text{Branch 2: } & (A_3, A_4) \\ \text{Branch 3: } & (A_4, A_5) \times (A_2, A_3) \\ \text{Branch 4: } & (A_3, A_4) \times (A_2, A_3) \end{aligned}$$

and dilute D_4 ,

$$\begin{aligned} \text{Branch 1: } & (D_4, A_6) \\ \text{Branch 2: } & (A_4, D_4) \\ \text{Branch 3: } & (D_4, A_6) \times (A_2, A_3) \\ \text{Branch 4: } & (A_4, D_4) \times (A_2, A_3) \end{aligned}$$

The isotropic expansions of these modular invariant partition functions are, to the relevant order,

$$\begin{aligned} (A_2, A_3) : \quad Z(q) &= q^{-\frac{1}{24}} \left[1 + q^{\frac{1}{8}} + q + 2q^{\frac{9}{8}} + 4q^2 + O\left(q^{\frac{17}{8}}\right) \right] \\ (A_3, A_4) : \quad Z(q) &= q^{-\frac{7}{120}} \left[1 + q^{\frac{3}{40}} + q^{\frac{1}{5}} + q^{\frac{7}{8}} + 2q^{\frac{43}{40}} + 3q^{\frac{6}{5}} + O\left(q^{\frac{15}{8}}\right) \right] \\ (A_4, A_5) : \quad Z(q) &= q^{-\frac{1}{15}} \left[1 + q^{\frac{1}{20}} + q^{\frac{2}{15}} + q^{\frac{1}{4}} + q^{\frac{4}{5}} + 3q^{\frac{21}{20}} + O\left(q^{\frac{17}{15}}\right) \right] \\ (A_4, D_4) : \quad Z(q) &= q^{-\frac{1}{15}} \left[1 + 2q^{\frac{2}{15}} + q^{\frac{4}{5}} + 4q^{\frac{17}{15}} + 2q^{\frac{4}{3}} + 4q^{\frac{9}{5}} + O\left(q^2\right) \right] \\ (D_4, A_6) : \quad Z(q) &= q^{-\frac{1}{14}} \left[1 + 2q^{\frac{2}{21}} + q^{\frac{2}{7}} + 2q^{\frac{20}{21}} + 4q^{\frac{23}{21}} + 2q^{\frac{9}{7}} + O\left(q^{\frac{10}{7}}\right) \right] \end{aligned}$$

The products of each of these with the Ising partition function $Z_I = (A_2, A_3)$ yield

$$Z_I \times (A_2, A_3) : \quad Z(q) = q^{-\frac{1}{12}} \left[1 + 2q^{\frac{1}{8}} + q^{\frac{1}{4}} + 2q + 6q^{\frac{9}{8}} + 4q^{\frac{5}{4}} + O\left(q^2\right) \right]$$

Model	Branch 1			Branch 2			N_{\max}
	Approx.	Exact		Approx.	Exact		
$A_3 \otimes A_3$	1.423	7/5	1.4	0.9991	1	1	8
$A_4 \otimes A_4$	1.606	8/5	1.6	1.3982	7/5	1.4	8
$[A_5, D_4] \otimes [A_5, D_4]$	1.712	12/7	1.714...	1.5930	8/5	1.6	6
$[A_{11}, D_7, E_6] \otimes [A_{11}, D_7, E_6]$	1.914	25/13	1.923...	1.8993	21/11	1.909...	6

Table 7. Central charges of the two-colour $C_2^{(1)}$ RSOS models. Here the notation $[G, G']$ means either G or G' .

Branch 1				Branch 2			
Approx.	Exact		Mult.	Approx.	Exact		Mult.
0.0749999	3/40	0.075	1	0.125999	1/8	0.125	1
0.200000	1/5	0.2	1	0.998457	1	1	1
0.874980	7/8	0.875	1	1.12489	9/8	1.125	2
1.07505	43/40	1.075	2	2.01084	2	2	2
1.20003	6/5	1.2	2	1.98828	2	2	2
1.19994	6/5	1.2	1	2.13060	17/8	2.125	2
1.87541	15/8	1.875	2				

Table 8. Scaling dimensions and multiplicities for the dilute A_3 model in the $u > 0$ branches.

Branch 3				Branch 4			
Approx.	Exact		Mult.	Approx.	Exact		Mult.
0.0778	3/40	0.075	1	0.1250	1/8	0.125	1
0.1270	1/8	0.125	1	0.1250	1/8	0.125	1
0.2033	1/5	0.2	1	0.2500	1/4	0.25	1
0.2401	1/5	0.2	1	1.0000	1	1	1
				1.0000	1	1	1
				1.1250	9/8	1.125	1
				1.1246	9/8	1.125	2
				1.1248	9/8	1.125	1
				1.1210	9/8	1.125	2
				1.2450	5/4	1.25	2
				1.2424	5/4	1.25	2
				1.9987	2	2	2
				1.9964	2	2	2
				1.9949	2	2	1

Table 9. Scaling dimensions and multiplicities for the dilute A_3 model in the $u < 0$ branches.

Branch 1				Branch 2			
Approx.	Exact		Mult.	Approx.	Exact		Mult.
0.050000	1/20	0.05	1	0.074999	3/40	0.075	1
0.013333	2/15	0.133...	1	0.199997	1/5	0.2	1
0.250000	1/4	0.25	1	0.873958	7/8	0.875	1
0.799969	4/5	0.8	1	1.075250	43/40	1.075	2
1.050060	21/20	1.05	2	1.199460	6/5	1.2	2
1.049920	21/20	1.05	1	1.196920	6/5	1.2	1
1.133360	17/15	1.133...	2				

Table 10. Scaling dimensions and multiplicities for the dilute A_4 model in the $u > 0$ branches.

Branch 3				Branch 4			
Approx.	Exact		Mult.	Approx.	Exact		Mult.
0.0501	1/20	0.05	1	0.07500	3/40	0.075	1
0.1256	1/8	0.125	1	0.12500	1/8	0.125	1
0.1357	2/15	0.133...	1	0.19985	1/5	0.2	1
0.1918	7/40	0.175	1	0.20000	1/5	0.2	1
0.2498	1/4	0.25	1	0.32500	13/40	0.325	1
				0.87506	7/8	0.875	1
				0.99984	1	1	1
				0.99803	1	1	1
				1.07508	43/40	1.075	1
				1.09886	43/40	1.075	2

Table 11. Scaling dimensions and multiplicities for the dilute A_4 model in the $u < 0$ branches.

Branch 1				Branch 2			
Approx.	Exact		Mult.	Approx.	Exact		Mult.
0.095234	2/21	0.095238...	2	0.13333	2/15	0.133...	2
0.285711	2/7	0.285714...	1	0.798273	4/5	0.8	1
0.951915	20/21	0.952381...	2	1.1335	17/15	1.133...	4
1.09586	23/21	1.09524...	4	1.32242	4/3	1.33...	2
1.28583	9/7	1.28571...	2	1.79266	9/5	1.8	2

Table 12. Scaling dimensions and multiplicities for the dilute D_4 model in the $u > 0$ branches.

Branch 3				Branch 4			
Approx.	Exact		Mult.	Approx.	Exact		Mult.
0.09603	2/21	0.09524...	2	0.12450	1/8	0.125	1
0.12520	1/8	0.125	1	0.13327	2/15	0.13333...	2
0.24414	37/168	0.22024...	1	0.25841	31/120	0.25833...	2
0.24414	37/168	0.22024...	1	0.80006	4/5	0.8	1
0.28376	2/7	0.28571...	1	0.92528	37/40	0.925	1
				0.99971	1	1	1
				1.13514	9/8	1.125	2
				1.11698	17/15	1.13333...	2

Table 13. Scaling dimensions and multiplicities for the dilute D_4 model in the $u < 0$ branches.

$$\begin{aligned}
Z_I \times (A_3, A_4) : \quad Z(q) &= q^{-\frac{1}{10}} \left[1 + q^{\frac{3}{40}} + q^{\frac{1}{8}} + 2q^{\frac{1}{5}} + q^{\frac{13}{40}} + q^{\frac{7}{8}} + q + O\left(q^{\frac{43}{40}}\right) \right] \\
Z_I \times (A_4, A_5) : \quad Z(q) &= q^{-\frac{13}{120}} \left[1 + q^{\frac{1}{20}} + q^{\frac{1}{8}} + q^{\frac{2}{15}} + q^{\frac{7}{40}} + q^{\frac{1}{4}} + q^{\frac{31}{120}} + O\left(q^{\frac{3}{8}}\right) \right] \\
Z_I \times (A_4, D_4) : \quad Z(q) &= q^{-\frac{13}{120}} \left[1 + q^{\frac{1}{8}} + 2q^{\frac{2}{15}} + 2q^{\frac{31}{120}} + q^{\frac{4}{5}} + q^{\frac{37}{40}} + q + 2q^{\frac{9}{8}} + O\left(q^{\frac{17}{15}}\right) \right] \\
Z_I \times (D_4, A_6) : \quad Z(q) &= q^{-\frac{19}{168}} \left[1 + 2q^{\frac{2}{21}} + q^{\frac{1}{8}} + 2q^{\frac{37}{168}} + q^{\frac{2}{7}} + O\left(q^{\frac{23}{56}}\right) \right]
\end{aligned}$$

We find that the results for the two-colour models are similar to those of the dilute models. The modular invariant partition functions are all found to be a product of two partition functions in Table 1 with the same central charge. Thus, for example, the partition functions of the two-colour model built on the graph $A_4 \otimes A_4$ are given by

$$\begin{aligned}
\text{Branch 1: } & (A_4, A_5) \times (A_4, A_5) \\
\text{Branch 2: } & (A_3, A_4) \times (A_3, A_4)
\end{aligned}$$

Our numerical estimates for the scaling dimensions of this model are summarised in Table 14. The expansions of the isotropic partition function products are

$$\begin{aligned}
\text{Branch 1: } \quad Z(q) &= q^{-\frac{2}{15}} \left[1 + 2q^{\frac{1}{20}} + q^{\frac{1}{10}} + 2q^{\frac{2}{15}} + 2q^{\frac{11}{60}} + 2q^{\frac{1}{4}} + q^{\frac{4}{15}} + 2q^{\frac{3}{10}} + O\left(q^{\frac{23}{60}}\right) \right] \\
\text{Branch 2: } \quad Z(q) &= q^{-\frac{7}{60}} \left[1 + 2q^{\frac{3}{40}} + q^{\frac{3}{20}} + 2q^{\frac{1}{5}} + 2q^{\frac{11}{40}} + q^{\frac{2}{5}} + 2q^{\frac{7}{8}} + 2q^{\frac{19}{20}} + O\left(q^{\frac{43}{40}}\right) \right]
\end{aligned}$$

Branch 1				Branch 2			
Approx.	Exact		Mult.	Approx.	Exact		Mult.
0.0499	1/20	0.05	2	0.0750	3/40	0.075	2
0.1016	1/10	0.1	1	0.1500	3/20	0.15	1
0.1333	2/15	0.133...	2	0.1996	1/5	0.2	2
0.1877	11/60	0.1833...	2	0.2750	11/40	0.275	2
0.2489	1/4	0.25	2	0.4000	2/5	0.4	1
0.2798	4/15	0.266...	1	0.8839	7/8	0.875	2
0.3107	3/10	0.3	2	0.9412	19/20	0.95	2
				1.0807	43/40	1.075	4

Table 14. Scaling dimensions and multiplicities for the two-colour $A_4 \otimes A_4$ model.

Similarly, in the case of the model built on $D_4 \otimes D_4$, the modular invariant partition functions are given by

$$\begin{aligned}
\text{Branch 1: } & (D_4, A_6) \times (D_4, A_6) \\
\text{Branch 2: } & (A_4, D_4) \times (A_4, D_4)
\end{aligned}$$

and in the case of the model built on $A_5 \otimes D_4$ by

$$\begin{aligned}
\text{Branch 1: } & (A_5, A_6) \times (D_4, A_6) \\
\text{Branch 2: } & (A_4, A_5) \times (A_4, D_4)
\end{aligned}$$

All of our numerical results are consistent with the conjectured modular invariant partition functions summarized in Section 1.

Acknowledgements

We thank Jean-Bernard Zuber for suggesting the principal conjecture of this paper and Omar Foda for numerous discussions. This research is supported by the Australian Research Council.

References

1. A. Cappelli, C. Itzykson and J.-B. Zuber, Nucl. Phys. **B280** (1987) 445; Comm. Math. Phys. **113** (1987) 1
2. V. Pasquier, Nucl. Phys. **B28** (1987) 162; J. Phys. A **20** (1987) L1229, 5707.
3. S. O. Warnaar, B. Nienhuis and K. A. Seaton, Phys. Rev. Lett. **69** (1992) 710.
4. Ph. Roche, Phys. Lett. **B4** (1992) 929.
5. S. O. Warnaar, P. A. Pearce, K. A. Seaton and B. Nienhuis, J. Stat. Phys. **74** (1994) 469.
6. S. O. Warnaar and B. Nienhuis, J. Phys. A **26** (1993) 2301.
7. A. A. Belavin, A. M. Polyakov and A. B. Zamolodchikov, Nucl. Phys. B **241** (1984) 333.
8. D. Friedan, Z. Qiu and S. Shenker, Phys. Rev. Lett. **52** (1984) 1575; in “Vertex Operators in Mathematics and Physics”, eds. J. Lepowsky, S. Mandelstam and I.M. Singer, Springer, 1984.
9. J. L. Cardy, Nucl. Phys. **B270** (1986) 186; Nucl. Phys. **B275** (1986) 200.
10. G. E. Andrews, R. J. Baxter and P. J. Forrester, J. Stat. Phys. **35** (1984) 193.
11. D. A. Huse, Phys. Rev. B **30** (1984) 3908.
12. S. O. Warnaar, M. T. Batchelor and B. Nienhuis, J. Phys. A **25** (1992) 3077
13. Y-K. Zhou and P. A. Pearce, Conformal Weights of Dilute A Lattice Models, in preparation (1995). Mechanics”,
14. D. Kim and P. A. Pearce, J. Phys. A **20** (1987) L451.
15. H. W. J. Blöte, J. L. Cardy and M. P. Nightingale, Phys. Rev. Lett. **56** (1986) 742; I. Affleck, Phys. Rev. Lett. **56** (1986) 746.